

The Identification of GIRK Channel Domains that Facilitate Rapid and Efficient Coupling to G Protein-Coupled Receptors

Daniele Young, Nicole Wydeven, and Kevin Wickman
Department of Pharmacology, University of Minnesota



Introduction

- G Protein-gated inwardly rectifying potassium channels (GIRK or Kir3) constitute one subfamily of K_{IR} potassium-selective ion channels.
 - The GIRK channel family consists of four mammalian subunits: GIRK1, GIRK2, GIRK3, GIRK4.
 - GIRK subunits combine to form homotetrameric or heterotetrameric complexes. Although, GIRK1 is unable to form a functional homotetrameric channel.
 - The GIRK1 subunit varies structurally from GIRK2, GIRK3, and GIRK4. The GIRK1 sequence lacks an ER export sequence, contains a unique phenylalanine pore residue, and has a unique distal C-terminal sequence.
 - GIRK channels are activated via a signal transduction cascade involving ligand-stimulated G Protein-coupled receptors (GPCRs), such as the GABA_B receptor.
 - GIRK1-containing channels exhibit robust GABA_B-evoked currents in the presence of baclofen, a GABA_B receptor agonist.
- GOAL:** To pinpoint key structural domains in the GIRK1 subunit that promote rapid and efficient coupling between neuronal GIRK channels and its neuronal GPCR prototype, the GABA_B receptor

Methods

Overlap Extension PCR (OE-PCR): To create an unbiased chimeric gene, a three-rounds of implication are required. Two separate reactions were placed in the thermocycler during the first round. A GIRK1 template was combined with 0.1 μL Hi-Fidelity Taq (Invitrogen Life Sciences, Carlsbad, CA), 10X Hi-Fidelity Taq buffer, 2.5 mM oligonucleotide mixture, 0.5 mM MgSO₄, and 2.5 mM dNTPs in a final volume of 50 μL. A GIRK2 template was combined with the same PCR mixture except with a different oligonucleotide mixture in a different tube. Both internal and external primers were used. The external primers used contain BamHI and XbaI restriction sites to allow for efficient molecular cloning. In addition, the C-terminal external primer contains an AUS epitope tag for biochemical assays. Internal primers varied based on the desired sequence of the chimera. The internal primers included a portion of complementarity to allow some overlap between GIRK1 and GIRK2. Each oligonucleotide mixture for round one OE-PCR contained an external primer to amplify the GIRK1 or GIRK2 template in one direction and an internal primer to amplify the sequence in the other direction. Amplified round one fragments were combined and placed back into the thermocycler without primers for round two, extending to form a complete double-stranded template. The third round of OE-PCR amplifies the round two product using the same external primers as in round one. PCR samples were subject to DNA electrophoresis on 1% agarose gels containing ethidium bromide for band visualization. The Eagle Eye system was used for visualization. A panel of chimeric constructs was created, each chimera containing a different combined sequence of GIRK1 and GIRK2.

Molecular biology. C-terminal AUS-tagged GIRK1 and GIRK2 chimeras: 1n2c-2, 2n1c-1, 2n1c-2, 2n1c-2 S148F, and 2n1c-3 S148F were generated by OE-PCR using Hi-Fidelity Taq as described above. Chimeric PCR fragments were incorporated into the pCR2.1-Topo vector according to manufacturer's protocols (Invitrogen Life Science, Carlsbad, CA) and inserts were sequenced in both directions for accuracy. Sequence verified fragments were then subcloned into the pcDNA3 expression plasmid.

Western blotting. HEK 293 cells were cultured according to ATCC specifications, and plated at 60-70% confluency in 6-well plates. Chimeric constructs were transfected into these cells by means of calcium phosphate transfection. Chimeric constructs were transfected with EGFP as a measure of transfection efficiency. Cells were harvested in 1 mL PBS and centrifuged (10,000rpm, 1min) two days after calcium phosphate transfection. The supernatant was carefully aspirated post centrifugation, and the cell pellet resuspended in 250μL 2x SDS sample buffer. Cells were lysed via sonication. 10ml of the sonicated mixture was combined with 2ml of 1M DTT (Fisher Scientific, Pittsburgh, PA). Prior to SDS-PAGE, samples were boiled at 100°C for 10min. 10 μL of each boiled sample was loaded onto 12% poly-acrylamide gel. A Tris-Glycine was used for SDS-PAGE. Samples were transferred to a nitrocellulose membrane (Thermo Scientific; Rockford, IL) after SDS-PAGE. Western blotting was performed using mouse anti-AUS antibody (Covance, Princeton, NJ) at 1:500 dilution. Donkey anti-mouse (LiCor, Lincoln, NE) was applied at 1:3,000 dilution for band visualization. Visualization was performed using the Odyssey Imaging System (LiCor, Lincoln, NE). Expression was observed for each chimeric construct at the corresponding size.

Immunoprecipitation with GIRK2. HEK 293 cells were cultured according to ATCC specifications, and plated at 60-70% confluency in 6-well plates. Chimeric constructs were transfected into these cells by means of calcium phosphate transfection. Chimeric constructs were transfected with EGFP as a measure of transfection efficiency. Cells were harvested in 1 mL PBS and centrifuged (10,000rpm, 1min) two days after calcium phosphate transfection. Cells were lysed in 0.5mL detergent buffer and homogenized by sonication. Detergent buffer contained: PBS+1% Triton, 150mM NaCl, and protease inhibitors. Cells were incubated on rocker for 20min at 4 °C. 40μL Protein G Agarose (Pierce) and 5μg rabbit anti-AUS (Bethyl Scientific; Montgomery, TX) on rocker for 20min at 4 °C. Cell homogenate centrifuged (14,000g, 15min) at 4 °C. Supernatant isolated and bead and anti-body mixture added. Incubated on rocker for 1hr at 4 °C. Washed beads three times with detergent buffer. Added 2x SDS sample buffer and 20μL DTT (Fisher Scientific; Pittsburgh, PA) and boiled for 5min. Samples then loaded onto a 12% poly-acrylamide gel for SDS-PAGE, transferred and immunoblotted with mouse anti-AUS (Covance, Princeton, NJ) and mouse anti-c-myc antibodies (Roche, Basel, Switzerland).

Biotinylation Assay. HEK 293 cells were cultured according to ATCC specifications, and plated at 60-70% confluency in 6-well plates. Chimeric constructs were transfected into these cells by means of calcium phosphate transfection. Chimeric constructs were transfected with EGFP as a measure of transfection efficiency. Cells washed three times with PBS. Added 550μL biotin solution to each well: 55μL 20mM NHS-PEG4-Biotin (Thermo Scientific; Rockford, IL) and 495μL PBS (pH8). Incubated with slow shaking for 1hr at 4 °C. Removed biotin and washed five times with PBS (pH8). Resuspended and lysed cells with detergent buffer: 1% Triton+protease inhibitors. Sonicated cells and incubated on rocker for 30min. Centrifuged cell homogenate (14000rpm, 15min). Isolated supernatant and added 30μL NeutraAvidin Agarose beads. Incubated on rotator for 30min at 4 °C. Pelleted beads and removed supernatant. Washed beads three times with detergent buffer. Eluted by adding 125μL 2X NuPage LDS sample buffer (Invitrogen Life Sciences, Carlsbad, CA). Added 25μL 1M DTT (Fisher Scientific; Pittsburgh, PA) and boiled for 5min. Samples then loaded onto a 12% poly-acrylamide gel for SDS-PAGE, transferred and immunoblotted.

Electrophysiology. HEK 293 cells were cultured according to ATCC specifications, plated on 8-mm glass coverslips (30,000 cells/coverslip), and transfected using Lipofectamine LTX (Life Technologies Corporation; Carlsbad, CA) with an EGFP expression plasmid (0.02 μg/coverslip) and either a chimeric construct. One day after transfection, whole-cell current were measured in EGFP-labeled cells with hardware (Axopatch-200B amplifier, Digidata 1320) and software (pCLAMP v. 9.0) from Molecular Devices, Inc. (Sunnyvale, CA). The bath solution consisted of (in mM): 140 NaCl, 4 KCl, 2 CaCl₂, 2 MgCl₂, 10 D-glucose, and 10 HEPES buffer, pH 7.4 with 10mM HEPES. Tyrode bath solution was added, producing larger currents. The high K⁺ bath solution consisted of (in mM): 120 NaCl, 25 KCl, 2 CaCl₂, 2 MgCl₂, 10 D-glucose, and 10 HEPES buffer, pH 7.4 with KOH. To probe the K⁺ selectivity of observed currents, bath solutions containing different external K⁺ concentrations were perfused onto the recorded cell using the SPT7B Fast-Stop Perfusion system (Warner Instruments, Inc., Hamden, CT). Upon achieving whole-cell access, cells were held at -70 mV to observe potassium currents. Cells were subjected to 0.2mM barium (Sigma-Aldrich; St. Louis, MO) to select for inwardly-rectifying potassium channels and 100μM baclofen (Sigma-Aldrich; St. Louis, MO). Baclofen is a GABA_B receptor agonist. All measured currents were filtered at 2 kHz and stored directly on hard disk for subsequent analysis.

Results

Figure 1: GIRK Channel Activation Mechanism

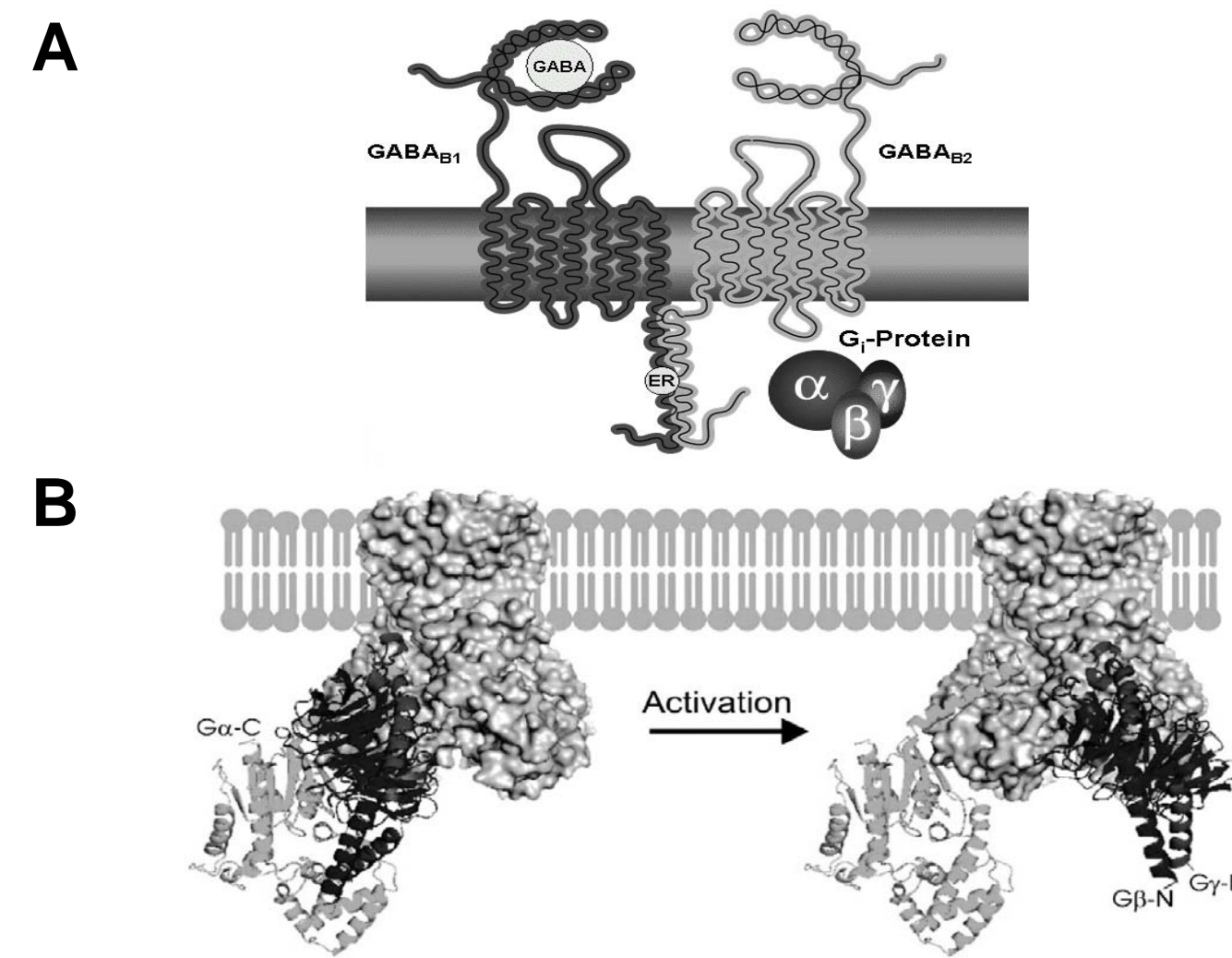


Figure 1. GIRK channel activation as a result of ligand-stimulated G Protein-coupled receptors
A) GABA_B receptor activation triggers a signal transduction cascade and GEF activity, allowing the G_{βγ} complex of the GPCR to interact with downstream effectors, including GIRK channels.¹¹
B) The dissociated G_{βγ} complex activates GIRK channels, increasing their gating and leading to the hyperpolarization of the cell membrane.¹²

Figure 2: GIRK1 and GIRK2 Chimeric Structures

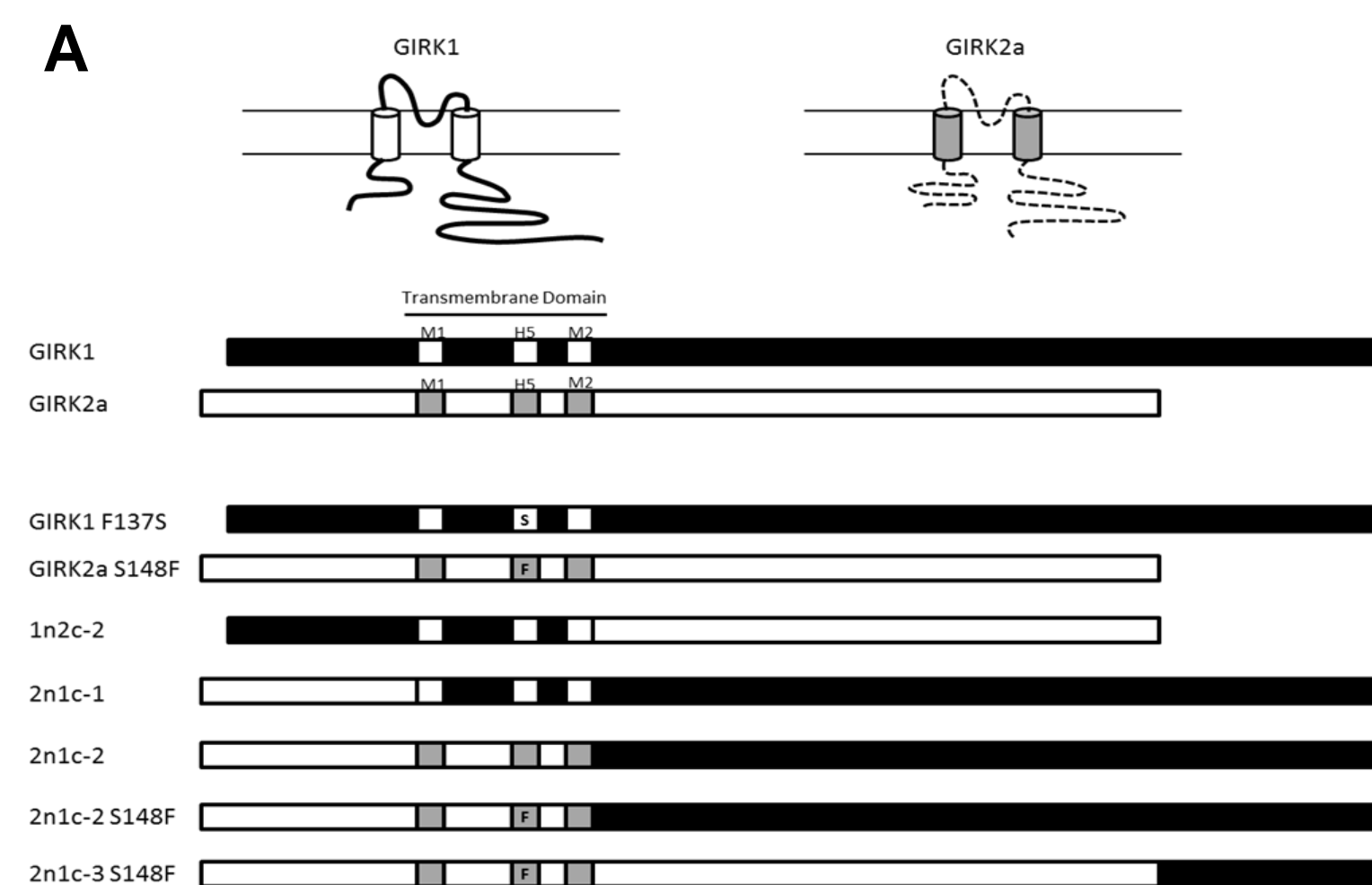


Figure 2. GIRK1 and GIRK2 containing chimeric panel.

A) Sequence location of GIRK1 and GIRK2 in each chimera. Black bars denote GIRK1 sequence. White squares correspond to GIRK1 transmembrane domains. White bars denote GIRK2 sequence, and the gray squares correspond to GIRK2 transmembrane domains. Gray boxes containing the letter "F" represent GIRK2 pore sequences containing the GIRK1 phenylalanine pore residue.

Figure 3: Biochemical Characterization of Chimeras

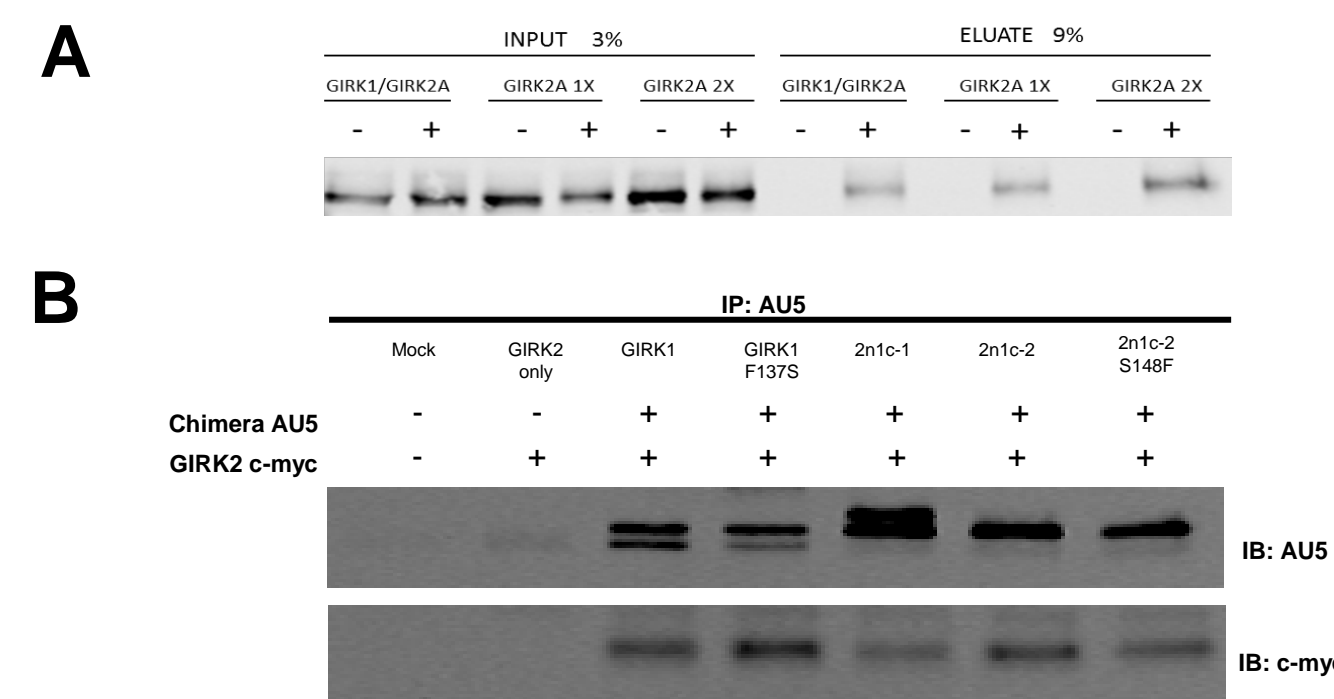


Figure 3. Biochemical characterization of GIRK1 and GIRK2 chimeric constructs.

A) Surface Biotinylation assay to assess changes of GIRK2 surface expression in the presence and absence of GIRK1. GIRK1 does not effect the level of GIRK2 at the membrane surface. B) Immunoprecipitation assay to assess chimeric channel formation with GIRK2. Each chimera was able to pull down GIRK2.

Figure 4: Functional Characterization of Chimeras

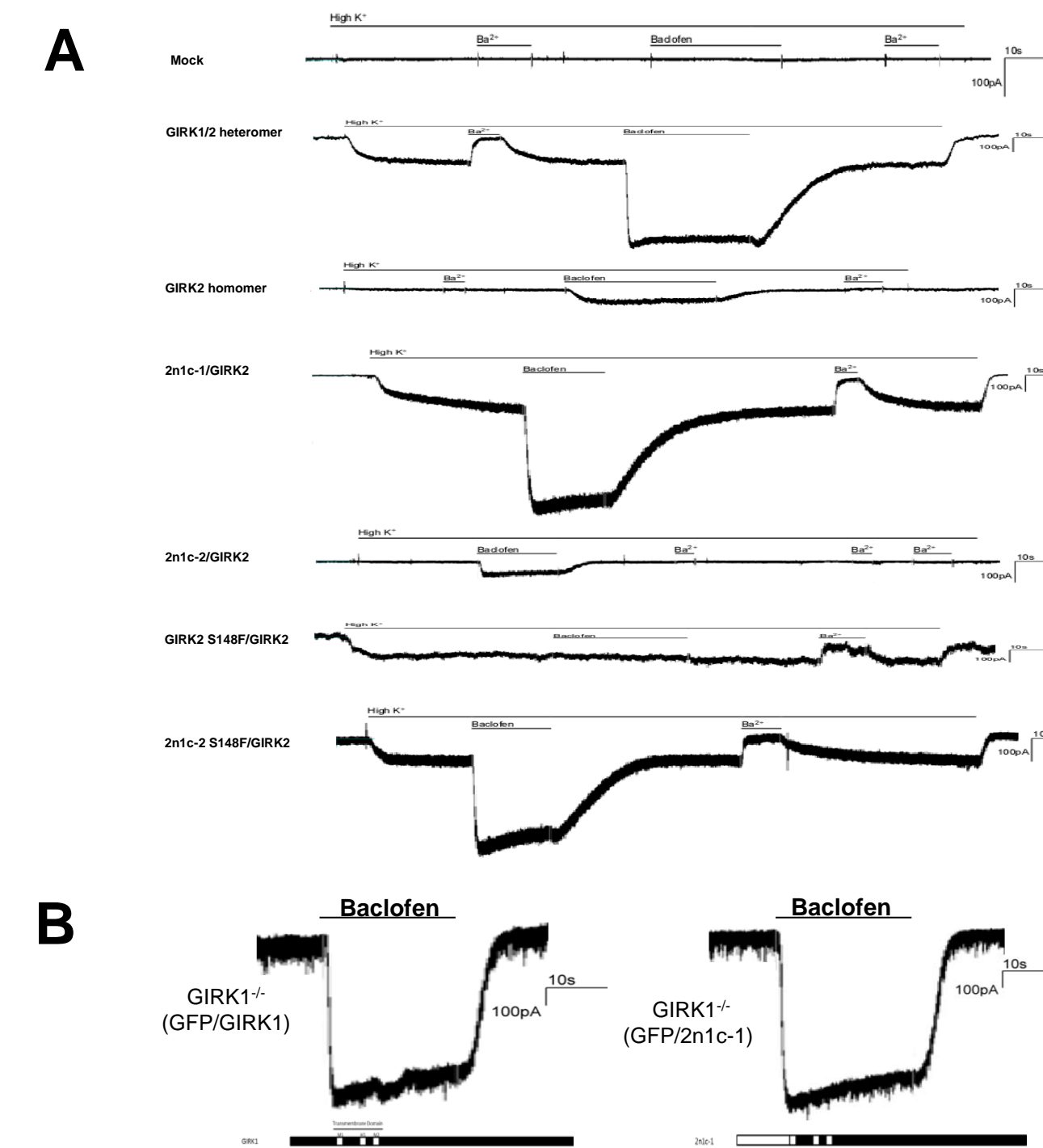


Figure 4. Functional characterization of GIRK1 and GIRK2 chimeric constructs.

A) Electrophysiology traces for the chimeric panel in response to Baclofen. B) The robust GABA_B receptor-evoked currents seen in the presence of GIRK1 can be rescued by transfecting GIRK1 knockout neurons from *mus musculus* with GIRK1 or a chimera containing the GIRK1 F137 pore residue and C-terminal sequence.

Conclusions

- All expressing chimeric constructs containing GIRK1 and GIRK2 are able to form a channel with GIRK2.
- The GIRK1 F137 pore residue is necessary to mediate robust GABA_B receptor-evoked currents.
- The C-terminal sequence of GIRK1 is also necessary to mediate robust GABA_B receptor-evoked currents.
- The robust GABA_B receptor-evoked currents are not due to differences in GIRK surface expression.
- The robust GABA_B receptor-evoked currents can be rescued in GIRK1 knockout hippocampal neurons from *mus musculus* by transfecting the neurons with GIRK1 or a chimeric construct containing the necessary structural features to mediate this effect.
- Our next steps are to further define the specific GIRK1 C-terminal sequence responsible for the functional difference observed in the presence of baclofen and to determine how these structural elements are mediating the robust receptor-induced currents.

References

1. Luscher C, Jan LY, Stoffel M, Malenka RC, Nicoll RA (1997) G protein-coupled inwardly rectifying K⁺ channels (GIRKs) mediate postsynaptic but not presynaptic transmitter actions in hippocampal neurons. *Neuron* [Erratum (1997) 19:945] 19: 687–695.
2. Marker CL, Luján R, Loh HH & Wickman K (2005). Spinal G-protein-gated potassium channels contribute in a dose-dependent manner to the analgesic effect of μ - and δ - but not κ -opioids. *J Neurosci* 25, 3551–3559.
3. Luscher, C., and P. A. Slesinger (2010). Emerging Roles for G Protein-gated Inwardly Rectifying Potassium (GIRK) Channels in Health and Disease. *Nat Rev Neurosci*. 11.5 (2010): 301-15. Print.
4. Arora D, Haluk DM, Kourich S, Praveitoni M, Fernández-Alacid L, Nicolau JC, Luján R, Wickman K (2010). Altered neurotransmission in the mesolimbic reward system of GIRK1 mice. *J Neurochem*. 2010 Sep 1;114(5):1487-97. Epub 2010 Jun 16
5. Fernández-Alacid L, Aguado C, Ciruela F, Martín R, Colón J, Cabañero MJ, Gassmann M, Watanabe M, Shigemoto R, Wickman K, Bettler B, Sánchez-Prieto J, Luján R (2009). Subcellular compartment-specific molecular diversity of pre- and post-synaptic GABA-activated GIRK channels in Purkinje cells. *J Neurochem*. 2009 Aug;110(4):1363-76. Epub 2009 Jun 22. Erratum in: *J Neurochem*. 2009 Sep;110(5):1715.
6. Koyrakh L, Luján R, Colón J, Karschin C, Kurachi Y, Karschin A, Wickman K (2005). Molecular and cellular diversity of neuronal G-protein-gated potassium channels. *J Neurosci*. 2005 Dec 7;25(49):11468-78.
7. Marker CL, Stoffel M, Wickman K (2004). Spinal G-protein-gated K⁺ channels formed by GIRK1 and GIRK2 subunits modulate thermal nociception and contribute to morphine analgesia. *J Neurosci*. 2004 Mar 17;24(11):2806-12.
8. Bettah I, Marker CL, Roman M, Wickman K (2002). Contribution of the Kir3.1 subunit to the muscarinic-gated atrial potassium channel IKACH. *J Biol Chem*. 2002 Dec 13;277(50):48282-8. Epub 2002 Oct 8.
9. Rusinova R, Shen YM, Dolios G, Padovan J, Yang H, Kirchberger M, Wang R, Logothetis DE (2009). Mass spectrometric analysis reveals a functionally important PKA phosphorylation site in a Kir3 channel subunit. *Pflügers Arch*. 2009 Jun;458(2):303-14. Epub 2009 Jan 17.
10. Praveitoni M, Wickman K (2008). Behavioral characterization of mice lacking GIRK/Kir3 channel subunits. *Genes Brain Behav*. 2008 Jul;7(5):523-31.
11. Brown, Steven. "UZH - Neuroparmacology - Introduction." UZH - Institute of Pharmacology and Toxicology - Institute of Pharmacology and Toxicology. 2 Dec. 2010. Web. 31 Mar. 2011. <http://www.pharma.uzh.ch/research/neuroparmacology/researchareas/signatransduction/introduction.html>.
12. Raveh, A (2009). Elucidation of the gating of the GIRK channel using a spectroscopic approach. *Journal of Physiology-London*. 2009 Nov 15;587(22):5331-5335.

Acknowledgements

Acknowledgements. The presenter thanks the principal investigator, Dr. Wickman, for this opportunity and his continual support. The presenter thanks the members of the Wickman laboratory, notably Nicole Wydeven for her tremendous assistance both experimentally and in the proof-reading of this poster.

Funding:

- NIH RO1 MH061933
- NIH P50 DA011806
- NIH R21029343 DA